Folding of the Multidomain Ribosomal Protein L9: The Two Domains Fold Independently with Remarkably Different Rates†

Satoshi Sato,‡ Brian Kuhlman,‡,§ Wen-Jin Wu,‡ and Daniel P. Raleigh*,‡,||

Department of Chemistry and Graduate Programs in Biophysics and in Molecular and Cellular Biology, State University of New York at Stony Brook, Stony Brook, New York 11794

Received December 23, 1998; Revised Manuscript Received February 17, 1999

ABSTRACT: The folding and unfolding behavior of the multidomain ribosomal protein L9 from *Bacillus stearothermophilus* was studied by a novel combination of stopped-flow fluorescence and nuclear magnetic resonance (NMR) spectroscopy. One-dimensional ^{1}H spectra acquired at various temperatures show that the C-terminal domain unfolds at a lower temperature than the N-terminal domain (T_m = 67 °C for the C-terminal domain, 80 °C for the N-terminal domain). NMR line-shape analysis was used to determine the folding and unfolding rates for the N-terminal domain. At 72 °C, the folding rate constant equals 2980 s^{-1} and the unfolding rate constant equals 640 s^{-1}. For the C-terminal domain, saturation transfer experiments performed at 69 °C were used to determine the folding rate constant, 3.3 s^{-1}, and the unfolding rate constant, 9.0 s^{-1}. Stopped-flow fluorescence experiments detected two resolved phases: a fast phase for the N-terminal domain and a slow phase for the C-terminal domain. The folding and unfolding rate constants determined by stopped-flow fluorescence are 760 s^{-1} and 0.36 s^{-1}, respectively, for the N-terminal domain at 25 °C and 3.0 s^{-1} and 0.0025 s^{-1} for the C-terminal domain. The Chevron plots for both domains show a V-shaped curve that is indicative of two-state folding. The measured folding rate constants for the N-terminal domain in the intact protein are very similar to the values determined for the isolated N-terminal domain, demonstrating that the folding kinetics of this domain is not affected by the rest of the protein. The remarkably different rate constants between the N- and C-terminal domains suggest that the two domains can fold and unfold independently. The folding behavior of L9 argues that extremely rapid folding is not necessarily functionally important.

The ribosomal protein L9 from *Bacillus stearothermophilus* (149 residues) has an unusual structure in which two globular domains are connected by a long α-helix. Both domains of L9 have a binding site for the 23S rRNA and it has been proposed that L9 acts as a molecular strut. The maintenance of the proper spacing and orientation of the two domains of L9 is important (*1*−*3*). A ribbon diagram of L9 is shown in Figure 1. The N-terminal domain (colored black) consists of a three-stranded antiparallel *β*-sheet packed between the central α-helix and a short α-helix. The C-terminal domain consists of two long loops, a short α-helix, and a three-stranded mixed *β*-sheet packed against the central α-helix. The long central α-helix (residues 41−74) is exposed to solvent in the middle and participates in the hydrophobic cores of the two domains at both ends. There is excellent evidence that this unusual architecture is preserved in solution (*1*, *4*).

Although the folding of single-domain proteins has been extensively studied (*5*−*8*), the folding and assembly of

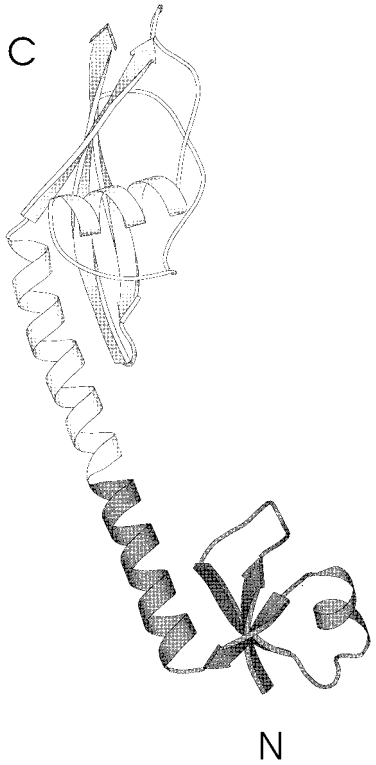

FIGURE 1: Ribbon diagram of L9 from *Bacillus stearothermophilus.* The isolated N-terminal domain studied by Kuhlman et al. (residues 1−56) consists of the shaded region (*12*, *13*). The program MOLSCRIPT (*27*) was used to create this diagram.

† This work was supported by a grant from NSF (MCB-9600866) to D.P.R., who is a Pew Scholar in the Biomedical Sciences. B.K. was partially supported by a graduate council fellowship from SUNY at Stony Brook.

* Author to whom correspondence should be addressed: Phone 516-632-9547; Fax 516-632-7960; Email DRaleigh@ccmail.sunysb.edu.

‡ Department of Chemistry.

§ Present address: Department of Biochemistry 357350, University of Washington, Seattle, WA 98195.

|| Graduate Programs in Biophysics and in Molecular and Cellular Biology.

10.1021/bi9830314 CCC: $18.00
Published on Web 04/08/1999

multidomain proteins is less well characterized. L9, in which two domains are connected by a rigid linker, provides an interesting system to investigate the folding behavior of a multidomain protein. The structure of L9 can be viewed as an intermediate case between multidomain proteins in which structurally independent domains are connected by flexible linkers and multidomain proteins in which domains interact extensively with each other (*9*−*11*). The two domains of L9 are expected to fold in the absence of the other, but their folding and stability may not be entirely independent. A peptide corresponding to the central helix of L9 was shown to be more than 85% helical below room temperature but less than 30% helical at 60 °C (*4*). Since the central helix of the intact L9 protein has been shown to be stable at 60 °C, it must be stabilized by interactions with the two terminal domains (*1*). The folding and stability of the isolated N-terminal domain of L9 was studied previously and was shown to fold rapidly by a two-state fashion (*12*, *13*).

In this study, the folding and unfolding of intact L9 were examined by the novel combination of two independent methods, stopped-flow fluorescence and nuclear magnetic resonance (NMR)[1] spectroscopy. L9 provides a simple and convenient system for folding studies since it does not contain disulfide bonds, does not bind to any metal ions or cofactors, and contains one tyrosine residue in each domain, which can be used to monitor the folding and unfolding process of each domain by spectroscopic methods. Folding kinetics are traditionally studied by stopped-flow or quenched-flow experiments. Nuclear magnetic resonance (NMR) spectroscopy can also provide kinetic information. The exchange rate for a system that undergoes intermediate to fast exchange may be determined by line-shape analysis (*12*, *14*), and the exchange rate for a system that undergoes slow exchange can be determined by a saturation transfer experiment (*15*−*17*). The temperature-dependent 1D ^{1}H NMR spectra of L9 acquired in this study show that the N-terminal domain undergoes fast exchange and that the C-terminal domain undergoes slow exchange; thus the rate constants for the two domains can be determined by line-shape analysis and saturation transfer experiments respectively. The analysis assumes a two-state folding model. However the stopped-flow fluorescence methods provide independent evidence that the folding of each of the domain is indeed two-state.

MATERIALS AND METHODS

Expression and Purification of L9. Bacillus stearothermophilus L9 was expressed and purified by the method described by Hoffman et al. (*3*). The *Escherichia coli* strains for the expression of L9 were generously provided by the Hoffman group.

Sample Preparation. All NMR samples were prepared in D_2O containing 1.8 mM L9, 20 mM sodium acetate-d_3, and 100 mM sodium chloride and were adjusted to the pH meter reading of 5.05 (pD apparent). All NMR samples also contain 0.3 mM 3-(trimethylsilyl)propionate (TSP) as an internal reference. All solutions for stopped-flow fluorescence were prepared in H_2O containing the same buffer used above (sodium acetate was used instead of sodium acetate-d_3) and adjusted to pH 5.45.

[1] Abbreviations: 1D, one dimensional; NMR, nuclear magnetic resonance; GdnHCl, guanidine hydrochloride; TSP, 3-(trimethylsilyl)-propionate.

Stopped-Flow Fluorescence. Stopped-flow fluorescence experiments were performed using an Applied Photophysics SX.18MV stopped-flow instrument at an excitation wavelength of 279 nm (±2.3 nm). Fluorescence signals above 305 nm were recorded with a cutoff filter. The temperature of the solutions and the flow circuit were maintained at 25.2 °C with a circulating water bath. For the folding experiments, approximately 600 μM of protein in 4.11 or 6.96 M guanidine hydrochloride (GdnHCl) was rapidly diluted against 10 volumes of 0.00−3.74 M GdnHCl. The final concentrations of GdnHCl varied from 0.37 to 2.99 M. A split time base was used to record both the fast phase and the slow phase in the same mixing experiment. For the unfolding experiments, approximately 600 μM protein in 0.00 M GdnHCl was rapidly mixed against 10 volumes of 1.37−6.96 M GdnHCl. The final concentrations of GdnHCl varied from 1.24 to 6.33 M. A single time base was used to record the two phases. The resulting traces were fit with two separate single-exponential functions for the folding experiments and fit with the sum of two exponential functions for the unfolding experiments to determine the observed rate constants. Each curve was obtained by averaging 9−12 individual measurements.

Nuclear Magnetic Resonance Spectroscopy. All 1D ^{1}H spectra of L9 were taken on a Varian Instruments Inova 500 MHz spectrometer. The temperatures were calibrated with an ethylene glycol standard.

Thermal Unfolding. A series of 1D ^{1}H spectra were recorded at temperatures between 25 °C and 90 °C to monitor the thermal unfolding of L9. 1D rather than 2D spectra were recorded in order to avoid excessive exposure to high temperature which can lead to deamidation of Asn residues. The plots of chemical shifts versus temperature or integrals versus temperature were fit to eq 1 with the program Sigma Plot (SPSS inc.) (*18*).

$$f(T) = \frac{a_N + \beta_N T + (\alpha_D + \beta_D T)\exp[-\Delta G^\circ_{D-N}(T)/RT]}{1 + \exp[-\Delta G^\circ_{D-N}(T)/RT]} \quad (1)$$

where

$$\Delta G^\circ_{D-N}(T) = \Delta H^\circ_{D-N}(T_m)\left(1 - \frac{T}{T_m}\right) - \Delta C^\circ_p\left[(T_m - T) + T\ln\left(\frac{T}{T_m}\right)\right] \quad (2)$$

f is the chemical shift or the peak integral, and T is temperature. α_N and β_N are the parameters that determine the chemical shifts of the native state, and α_D and β_D are those for the denatured state. α and β correspond to a y-intercept and a slope of a line, respectively. T_m is the temperature at the transition midpoint. There are seven adjustable parameters in the fit. However, the shape of the curves is largely independent of the value of ΔC°_p. The peak from the ϵ protons of Tyr 25 and the methyl resonances of Met 1 were used to construct the denaturation curves of the N-terminal domain. The intensity of the peak at 6.0 ppm, which is due to the δ2 proton on His 144 in the C-terminal domain, and the relative intensities of the Tyr 126 peaks coming from the unfolded state (6.8 ppm) and the folded

state (6.4 ppm) were used to determine the T_m for the C-terminal domain.

Line-Shape Analysis. The folding and unfolding rates of the N-terminal domain were determined by NMR line-shape analysis of resolved resonances that were broadened due to chemical exchange *(12, 14, 19).* The analysis assumes a two-state exchange process. Stopped-flow fluorescence measurements demonstrate that this is a valid assumption. The intensity of a peak as a function of frequency, $I(\upsilon)$, is related to the folding and unfolding rate constants, k_f and k_u, the relative populations of the native and denatured states, p_N and p_D, and the chemical shifts of the native and denatured proteins, υ_N and υ_D, by the following equations:

$$I(\upsilon) = C_0 \frac{\left\{P\left[1 + \tau\left(\frac{p_D}{T_{2,N}} + \frac{p_N}{T_{2,N}}\right)\right] + QR\right\}}{P^2 + R^2} \qquad (3)$$

where

$$P = \tau[(1/T_{2,N}T_{2,D}) - 4\pi^2(\Delta\nu)^2 + \pi^2(\delta\nu)^2] + (p_N/T_{2,N}) + (p_D/T_{2,D})$$

$$R = 2\pi\Delta\nu\{1 + \tau[(1/T_{2,N}) + (1/T_{2,D})]\} + \pi\delta\nu\tau[(1/T_{2,N}) - (1/T_{2,D})]\pi\delta\nu\,(p_N - p_D)$$

$$Q = \tau[2\pi\Delta\nu - \pi\delta\nu(p_N - p_D)]$$

$$\delta\nu = \nu_N - \nu_D \quad \Delta\nu = [(\nu_N + \nu_D)/2] - \nu$$

$$\tau = 1/(k_u + k_f) \qquad p_N = k_f\tau \qquad p_D = k_u\tau$$

C_0 is a normalizing constant that is proportional to the protein concentration used in the experiment. $T_{2,N}$ and $T_{2,D}$ are the apparent transverse relaxation times for the native and denatured protein, respectively. The peak from the ϵ protons of Tyr 25 in the spectra recorded at 67.6, 72.1, 76.6, and 81.4 °C were fit to eq 3 with the program Sigma Plot to determine τ, C_0, and p_N as described previously (*12*). The other parameters (υ_N, υ_D, $T_{2,N}$, and $T_{2,D}$) were obtained from the spectra of the native and denatured proteins. The value of $T_{2,N}$ and $T_{2,D}$ were determined from measurements of the line widths of the folded and unfolded resonances.

Saturation Transfer Experiments. The folding and unfolding rate constants of the C-terminal domain were determined by saturation transfer experiments performed at 69.0 °C (*20*). A selective pulse prior to the observation pulse was used to saturate the resonance of interest. The effects of the perturbation were measured by integrating a resolved peak in a normal 1D ^{1}H spectrum or by integrating a peak in a 1D ^{1}H difference spectrum. The peaks from the ϵ protons on Tyr 126 (6.4 and 6.8 ppm) and the δ2 proton on His 144 in the C-terminal domain (6.0 ppm) were used to determine the folding and unfolding rate constants for the C-terminal domain. The corresponding peak from the unfolded state was identified by difference spectroscopy. The longitudinal relaxation times (T_1) were obtained separately by inversion recovery experiments except for the T_1 of the His 144 resonance from the unfolded protein, which was not resolved and was assumed to be the same as the T_1 of the folded resonance. It was possible to independently measure the T_1s for other resonances in the folded state and unfolded state and they were found to differ by less than the experimental uncertainty (see Results). This indicates that the assumption of equal T_1 values for the folded and unfolded resonances of His 144 is reasonable. If the exchange rate between the folded and unfolded state of a protein is slow on the NMR time scale, two distinct resonances, one from the folded state (the F resonance), and the other from unfolded state (the U resonance), are observed near the midpoint of the transition (*21*). If the F resonance is selectively saturated, the intensity of the U peak will decrease from its unperturbed value, I_0, toward a new limiting value, I_∞. The ratio of the two values are given by the folding rate k_f and the apparent longitudinal relaxation time $T_{1,U}$ by (*17*, 20)

$$\frac{I_0}{I_\infty} = 1 + k_f T_{1,U} \qquad (4)$$

and the rate of the intensity decrease is given by

$$\frac{\mathrm{d}\ln|I_\infty - I|}{\mathrm{d}t} = -\left(k_f + \frac{1}{T_{1,U}}\right) \qquad (5)$$

The intensity of the U peak versus saturation time was fit to eq 5 to obtain k_f. The unfolding rate constant can be obtained by the complementary experiment in which the U resonance is saturated and the intensity of the F resonance is recorded. The analysis assumes two-state exchange.

Error Analysis. The error in the parameters obtained by nonlinear regression was determined by using the method described by Shoemaker et al. (*22*). Nonlinear regressions were repeated holding one of the parameters constant. The χ^2 value calculated from the new regression was then compared to the χ^2 value from the best fit by using an *F*-test to determine the 95% confidence limit. The upper and lower limits for each parameter were obtained in this manner. The error in a parameter obtained from a nonlinear regression is not necessarily symmetric.

RESULTS

Thermal Unfolding Monitored by NMR. The equilibrium thermal unfolding transitions were monitored by following resolved peaks in a set of 1D ^{1}H spectra (Figure 2). The peak assignments from Kuhlman et al. (*12*) and Hoffman et al. (*2*) were used to identify the resolved resonances. The peak at 6.0 ppm is from the δ2 proton on His 144 (all three histidines are located in the C-terminal domain), and the peak at 6.4 ppm is from the ϵ protons on Tyr 126. All of these residues are located in the C-terminal domain. The peaks at 6.5 and 7.5 ppm are from the ϵ and δ protons on Tyr 25 and Phe 5, respectively, which are located in the N-terminal domain. Resonances due to Met 1 could also be followed throughout the transition. The temperature dependence of the spectra clearly demonstrates different unfolding behaviors for the N-terminal domain and the C-terminal domain. The disappearance of the peak from the ϵ protons on Tyr 126 (6.4 ppm) around 70 °C suggests that the C-terminal domain unfolds first. The integral of the His 144 peak and the relative intensity of the Tyr 126 peak coming from the folded and the unfolded state were plotted as a function of temperature and fit to eq 1 to obtain the T_m for the C-terminal domain. The results are as follows: T_m = 66.4 °C (−3.5, +2.9) for His 144; T_m = 67.3 °C (−0.9, +0.9) for Tyr 126 (the

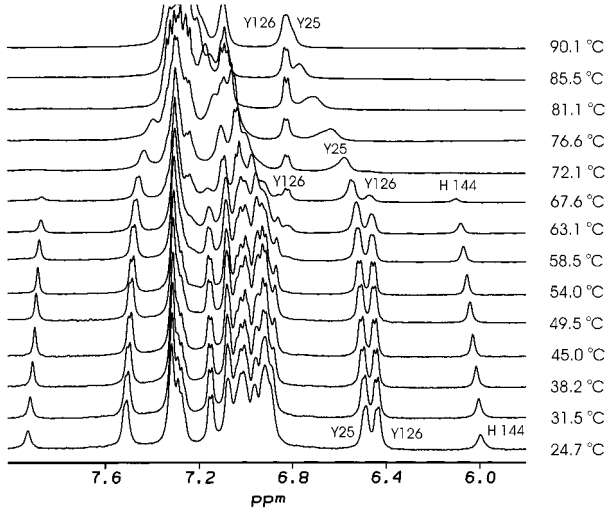

FIGURE 2: One-dimensional ^{1}H spectra of L9 at various temperatures in 20 mM sodium acetate and 100 mM sodium chloride, 100% D_2O, pD 5.05 (apparent). Tyr 25 is located in the N-terminal domain. Tyr 126 is in the C-terminal domain.

numbers in parentheses represent the 95% confidence limit). The chemical shifts of the methyl group on Met 1 and of the ϵ protons on Tyr 25 were plotted as a function of temperature and fit to eq 1 to obtain the midpoint of the transition for the N-terminal domain. The results are as follows: $T_m = 80.3$ (−1.6, +2.4) °C for Met 1; $T_m = 80.4$ (−1.3, +1.8) °C for Tyr 25. These values show good agreement with each other and with the values determined for the isolated N-terminal domain under the same conditions ($T_m = 81.0 \pm 1.5$ °C) (*23*). The unfolding was 90% reversible at 500 μM. The thermal unfolding curves are shown in Figure 3.

The observation of separate resonances from the folded and unfolded C-terminal domain indicates that the exchange rate of the C-terminal domain is slow on the NMR time scale. On the other hand, the resonances from the N-terminal domain shift and become broad in the transition region. This peak pattern indicates that the exchange of the N-terminal is intermediate to fast on the NMR time scale.

Measurement of the Folding and Unfolding Rates of the N-Terminal Domain by Line-Shape Analysis. The resonances due to Tyr 25 can be used for line-shape analysis to determine the folding and unfolding rates for the N-terminal domain. The results are listed in Table 1. To estimate the error associated with the analysis, the line-shapes were simulated by various combinations of folding rates and unfolding rates, and the residuals were compared to the experimental spectrum (*12*, *14*). This analysis (Figure 4) shows that the residuals become large if one of the rates is changed by 13%. If k_f and k_u are both varied such that the equilibrium constant remains fixed, then the residuals become large if both rates are changed by 13%. The N-terminal domain folds very rapidly with a rate constant of 2980 s^{-1} at 72.1 °C, pD 5.05 (apparent), which is similar to the folding rate constant, 2690 s^{-1}, determined for the isolated N-terminal domain under the same buffer conditions at 72.7 °C (*13*).

Determination of the Folding and Unfolding Rates of the C-Terminal Domain by Saturation Transfer Experiments. The folding and unfolding rate constants for the C-terminal

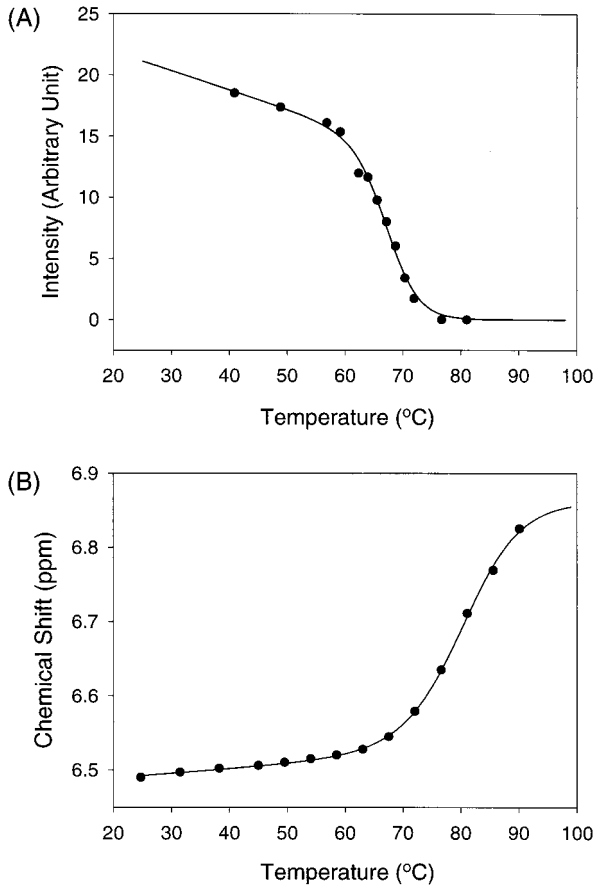

FIGURE 3: Thermal denaturation of L9 followed by NMR. One-dimensional ^{1}H spectra of L9 were recorded at various temperatures in 20 mM sodium acetate and 100 mM sodium chloride, 100% D_2O, pD 5.05 (apparent). (A) Unfolding of the C-terminal domain followed by monitoring a resonance due to Tyr 126. The curve shows the best fit to eq l giving a T_m of 67.3 °C. (B) Unfolding of the N-terminal domain followed by monitoring a resonance due to Tyr 25. The curve represents the best fit to eq 1 giving a T_m of 80.4 °C.

Table 1: Folding and Unfolding Rate Constants for the N-Terminal Domain in Intact L9[a]

temperature (°C)	k_f (s^{-1})	k_u (s^{-1})
67.6	3950	310
72.1	2980	640
76.6	1820	1100
81.1	1390	1770

[a] The folding and unfolding rate constants were derived from NMR line-shape analysis of the Tyr 25 resonances. All experiments were conducted at pD 5.05 (apparent).

domain were determined by saturation transfer experiments performed at 69.0 °C. In order to measure rates by saturation transfer experiments, it is necessary to know the T_1 of the resonances of interest. The apparent T_1 values for the peaks at 6.0, 6.4, and 6.8 ppm were determined by performing inversion recovery experiments. The results are 1.07 s (−0.45, +0.64) for the folded His 144 peak at 6.0 ppm, 1.41 s (−0.35, +0.41) for the 6.4 ppm peak, which is due to the folded Tyr 126, and 1.28 s (−0.42, +0.58) for the 6.8 ppm peak, which arises from unfolded Tyr 126. The apparent T_1 of the His 144 peak in the unfolded state was not determined because the peak is buried in a cluster of peaks and was assumed to be the same as that of the peak due to the folded form. The assumption seems reasonable given the close

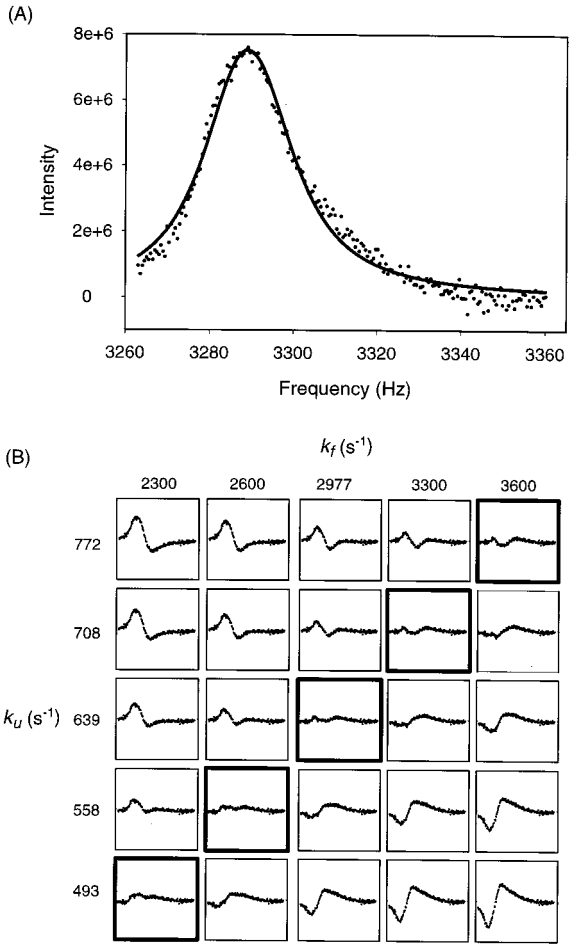

FIGURE 4: Line-shape analysis of the resonance from the ϵ protons of Tyr 25 at 72.1 °C. (A) Observed spectrum (dots) and the simulated spectrum that shows the best fit. (B) Residuals between the observed spectrum and the simulated spectra obtained with different combinations of k_f and k_u. The residuals shown along the diagonal (bold squares) correspond to simultaneously varying k_f and k_u such that the equilibrium constant does not change.

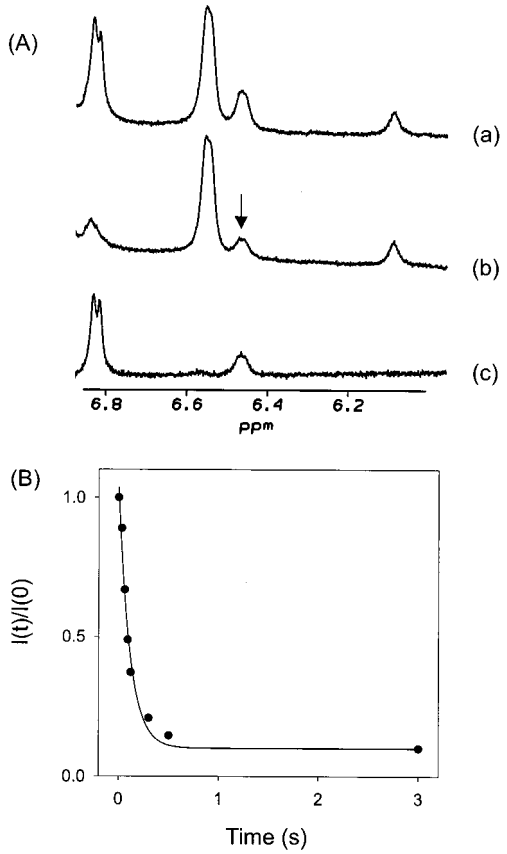

FIGURE 5: (A) Portion of the ^{1}H NMR spectra of L9 recorded at 69.0 °C. Spectrum a is a control spectrum in which a presaturation pulse was applied at the frequency where there are no resonances. Spectrum b was recorded with a presaturation pulse applied for 90 ms at the resonance indicated by an arrow (the Y126 resonance in the folded state). The intensity of the resonance at 6.8 ppm (the Y126 resonance in the unfolded state) decreases due to saturation transfer. The difference spectrum [a − b] is shown at the bottom (spectrum c). (B) Time development of the saturation transfer from the 6.4 ppm resonance to the 6.8 ppm resonance. $I(t)$ is the intensity at time t and $I(0)$ is the initial intensity. The curve shows the best fit to eq 5, which gives an unfolding rate of 8.2 s^{-1} for the C-terminal domain.

agreement between the apparent T_1s for the folded and unfolded resonances of Tyr 126. Furthermore, the calculated rate is insensitive to the exact choice of T_1. The folding rate constants determined by use of the 6.0 ppm peak and the 6.4 ppm peak are 3.3 s^{-1} (−1.7, +2.8) and 3.4 s^{-1} (−1.3, +2.0), respectively (the numbers in parentheses represent the 95% confidence limit). The unfolding rate constants measured by use of the 6.0 ppm peak and the 6.4 ppm peak were found to be 9.8 s^{-1} (−5.3, +7.3) and 8.2 s^{-1} (−3.6, +4.5) respectively. Changing the values of T_1 within the uncertainty ranges does not change the values of the folding and unfolding rate constants significantly. A representative saturation transfer curve is shown in Figure 5.

Stopped-Flow Fluorescence Measurements of Folding and Unfolding Rates. The experimental traces of fluorescence intensity versus time obtained with stopped-flow experiments show two separate exponential traces, one growing rapidly upon folding and one decaying slowly upon folding. In unfolding experiments, an initial rapid decrease in fluorescence is observed, followed by a slow increase. Since fluorescence measurements provide only global information about the system, the origin of the two exponential traces cannot, in principle, be interpreted directly at the molecular level. Intermediates could form rapidly and the two domains could fold simultaneously. Alternatively, the two different phases could arise from the independent folding of each domain. The NMR experiments provide direct evidence that the folding of the N-terminal domain is fast and the folding of the C-terminal domain is slow. This suggests that the fast fluorescence phase is due to the folding of the N-terminal domain. Further evidence in support of these assignments comes from fluorescence-monitored equilibrium unfolding experiments. When the isolated N-terminal domain folds, an increase in fluorescence is observed. When the C-terminal domain in the intact protein folds, a decrease in fluorescence is observed. Tyr 25 is the sole fluorophore in the N-terminal domain. Tyr 126 is the only fluorophore in the C-terminal domain and in the folded structure is located close to His 144, which presumably quenches the folded-state fluorescence. In the kinetic folding experiments, an initial rapid increase in fluorescence intensity is observed, followed by a subsequent slow decrease in intensity. These intensity changes are fully consistent with the equilibrium measurements. With this information, the fast exponential phase is assigned to the N-terminal domain and the slow phase is assigned to the C-terminal domain. This assignment is also

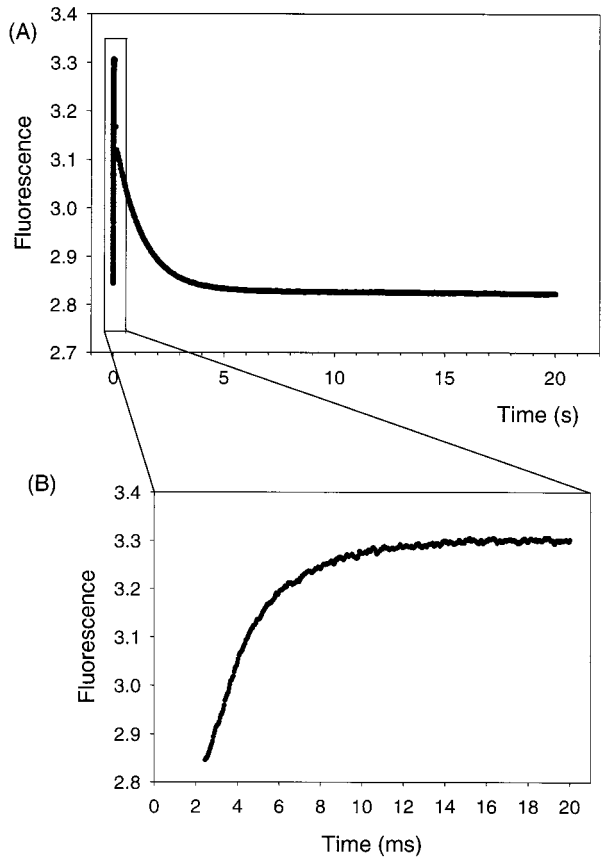

FIGURE 6: Representative folding traces from the stopped-flow fluorescence experiments performed at 25.2 °C. The final GdnHCl concentration was 0.47 M for these traces. (A) Complete trace. (B) Expansion of the initial portion of trace A. The traces are well fit to a single-exponential function.

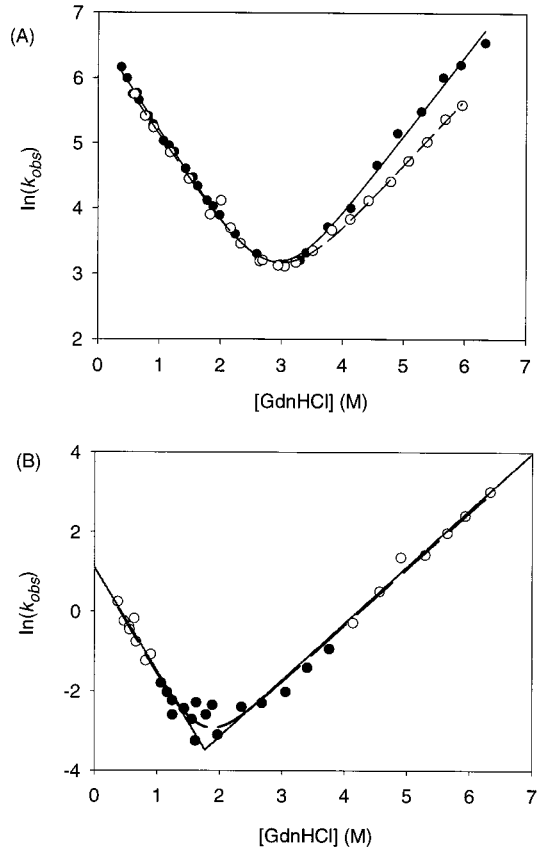

FIGURE 7: Chevron plots derived from the stopped-flow fluorescence experiments performed at 25.2 °C. (A) N-Terminal domain in the intact L9 (●) and isolated N-terminal domain (○). The curve shows the best fit to eq 6, giving a k_f of 760 s^{-1} and a k_u of 0.36 s^{-1} for the intact N-terminal domain and a k_f of 720 s^{-1} and a k_u of 0.75 s^{-1} for the isolated N-terminal domain. (B) C-Terminal domain. The data points below 1.0 M GdnHCl and above 4.0 M GdnHCl (○) were used for linear regression. The lines are the resulting best fits that give a k_f of 3.00 s^{-1} and a k_u of 0.0025 s^{-1}. The curve (broken line) shows the best fit of the entire data set to eq 6.

consistent with the fast increase in fluorescence observed in folding experiments with the isolated N-terminal domain (*13*). A representative trace for the folding reaction is shown in Figure 6.

The large difference in the time constants of the two phases allows apparent rate constants for the N-terminal and the C-terminal domain to be determined with a high degree of confidence. Plots of the natural logarithm of the observed rate constants (k_{obs}) versus GdnHCl concentration for both the N-terminal and the C-terminal domain show a characteristic V-shaped curve (a so-called "Chevron plot") that is indicative of two-state folding (Figure 7). Deviation from linearity, rollover, at low GdnHCl concentration, which is suggestive of the formation of intermediates, was not observed. There is some scatter in the data collected near the midpoint of the folding transition of the C-terminal domain. This probably arises because the change in fluorescence intensity is very small under these conditions.

The plots of ln k_{obs} versus GdnHCl concentration ([GdnHCl]) were fit to the following equation to determine the folding and unfolding rate constants in the absence of GdnHCl [k_f (0 M GdnHCl) and k_u (0 M GdnHCl)]:

$$\ln k_{obs} = \ln[k_f(0\text{ M GdnHCl})\exp(m_f\,[\text{GdnHCl}]/RT) + k_u(0\text{ M GdnHCl})\exp(m_u\,[\text{GdnHCl}]/RT)] \quad (6)$$

where m_f and m_u are constants that describe how k_f and k_u vary as a function of the concentration of GdnHCl. At 25.2 °C in H_2O, the folding rate constant for the N-terminal domain is 760 s^{-1} (−140, +180) and the unfolding rate constant for the N-terminal domain is 0.36 s^{-1} (−0.18, +0.28). The apparent stability of the N-terminal domain calculated from these rate constants is 4.53 kcal mol^{-1} (−0.32, +0.36). The equilibrium m value calculated from m_f and m_u ($m = m_u - m_f$) is 1.58 kcal mol^{-1} M^{-1} (−0.08, +0.09) and the value of θ_m [$m_f/(m_u - m_f)$] is 0.54 (−0.05, +0.05). The m value is related to the change in solvent-accessible surface area upon folding (*24*). The value of θ_m provides a measure of the fraction of the surface area buried in the folded state that is buried in the transition state (*25*). A θ_m of 0.54 indicates that 54% of the surface area that is buried in the folded state is buried in the transition state; thus, the transition state of the N-terminal domain is relatively open (*5*). The stability, the m value, and the θ_m value for the isolated N-terminal domain have been previously determined to be 4.06 kcal mol^{-1} (−0.41, +0.45), 1.46 kcal mol^{-1} M^{-1} (−0.11, +0.11), and 0.60 (−0.07, +0.07) at 25.0 °C (B. Kuhlman, unpublished data). The stability and the m value are similar to the values for the N-terminal domain in the intact protein. This similarity indicates that the folding of the N-terminal domain is not significantly affected by the rest of the protein.

For the folding and unfolding rate constants of the C-terminal domain, the plot of ln k_{obs} versus [GdnHCl] was fit by linear regression for the values of [GdnHCl] below 1.0 M and above 4.0 M in order to avoid possible errors from the scattering of the data at the bottom of the curve. The folding and unfolding rate constants for the C-terminal domain in the absence of denaturant were determined to be 3.00 s^{-1} (2.18, +8.00) and 0.0025 s^{-1} (−0.0023, +0.026). The rate constants obtained by fitting the entire curve to eq 6 were almost identical (k_f = 3.02 s^{-1}, k_u = 0.0025 s^{-1}). The stability, the *m* value, and the θ_m value for the C-terminal domain were calculated to be 4.23 kcal mol^{-1} (−0.72, +0.80), 2.45 kcal mol^{-1} M^{-1} (−0.50, +0.71), and 0.65 (−0.13, +0.12), respectively. The θ_m of 0.65 suggests that the transition state for the folding of the C-terminal domain is more compact than that of the N-terminal domain.

DISCUSSION

The Two Domains Fold Independently. The NMR studies and the stopped-flow experiments show that the folding and unfolding rate constants for the N-terminal domain are greater than those measured for the C-terminal domain by 2 or 3 orders of magnitude. These results suggest that the folding and unfolding of the N-terminal domain and the C-terminal domain are independent of each other. The plot of ln *k* versus [GdnHCl] shows that the folding transition of the each domain can be described by a two-state mechanism. The folding behavior of L9 has some interesting implications for arguments which suggest that the ability to fold very rapidly may be physiologically important and may even be evolutionary conserved (*14*, *26*). The N-terminal domain, both in isolation and in the context of the intact protein, folds extremely rapidly. Indeed, it is one of the fastest folders studied to date. However, this is almost certainly physiologically irrelevant at least in regard to RNA binding. For L9 to function and fulfill its biological role, both domains must be folded. We have demonstrated that the folding rate of the C-terminal domain is more than 2 orders of magnitude slower than that of the N-terminal domain. On the other hand, the two domains of L9 have a similar stability. Thus the rapid folding of the N-terminal domain, while physically very interesting, is not likely to have any direct relevance for RNA binding although it might, perhaps, play a role in protecting the N-terminal domain from proteolysis.

Folding and Stability of the N-Terminal Domain in L9 and the Isolated N-Terminal Domain. The thermal stability of the N-terminal domain in the intact protein and the isolated N-terminal domain are almost the same. The T_m of the N-terminal domain in the intact protein is 80.3 °C while the T_m of the isolated N-terminal domain is 81.0 °C at pD 5.05 (apparent) in D_2O (*23*). The folding rate of the N-terminal domain in the intact protein and the isolated N-terminal domain are also similar [760 s^{-1} (−140, +180) and 720 s^{-1} (−190, +280)] at 25 °C, while the unfolding rate of the N-terminal domain in intact L9 is about half the unfolding rate of the isolated N-terminal domain [0.36 s^{-1} (−0.18, +0.28) and 0.75 s^{-1} (−0.39, +0.74)]. The similarity in k_f and the difference in k_u suggest that the folded state of the intact N-terminal domain is slightly stabilized by the rest of the protein. A similar result was observed with the comparison of the isolated N-terminal domain (residues 1−56) to a truncated version of the isolated N-terminal domain (residues 1 −51) (D. L. Luisi, B. Kuhlman, K. Sideras, P. A. Evans, and D. P. Raleigh submitted for publication). In this study, truncation of the final helix of the isolated N-terminal domain (the start of the long central helix in the intact protein) led to no measurable change in the folding rate but did affect the unfolding rate (Table 2).

Table 2: Comparison of the Kinetic Parameters for the N-Terminal Domains in the Intact Protein, the Isolated N-Terminal Domain (1−56), and the Truncated Version of the Isolated N-terminal Domain (1−51)[a]

	N-terminal domain in the intact protein in H_2O	isolated N-terminal domain (1−56) in H_2O	isolated N-terminal domain (1−56) in D_2O	isolated N-terminal domain (1−51) in D_2O
k_f (s^{-1})	760 (−140, +180)	720 (−190, +280)	1053 (−277, +213)	942 (−328, +235)
k_u (s^{-1})	0.36 (−0.18, +0.28)	0.75 (−0.39, +0.74)	0.55 (−0.40, +0.24)	6.50 (−2.0, +1.7)
$\Delta G°$ (kcal mol^{-1})	4.53 (−0.32, +0.36)	4.06 (−0.41, +0.45)	4.47 (−0.5, +0.5)	2.95 (−0.18, +0.20)
m (kcal mol^{-1} M^{-1})	1.58 (−0.08, +0.09)	1.46 (−0.11, +0.11)	1.47 (−0.14, +0.14)	1.49 (−0.08, +0.08)
θ_m	0.54 (−0.05, +0.05)	0.60 (−0.07, +0.07)	0.59 (−0.05, +0.05)	0.71

[a] All experiments were performed at 25 °C in H_2O or D_2O, 20 mM sodium acetate, 100 mM NaCl, pH 5.45 or pD 5.05 (apparent). The data for the isolated N-terminal domain (1−56) were obtained from Kuhlman et al. (*23*). The data for the 1−51 variant were taken from Luisi, Kuhlman, Sideras, Evans, and Raleigh (submitted for publication). The numbers in parentheses represent the 95% confidence limit.

In conclusion, the N-terminal domain and the C-terminal domain of L9 fold and unfold independently, each by an apparent two-state mechanism. The stability and folding behavior of the isolated N-terminal domain is similar to that of the intact N-terminal domain. This study demonstrates the power of combining stopped-flow experiments with NMR experiments. Stopped-flow provides direct information on kinetic events including formation of kinetic intermediates, but it provides only a global view of the folding process. In the absence of additional information, it can be difficult to assign the observed phases to specific molecular events. On the other hand, NMR studies can provide specific information, but since the analysis assumes two-state exchange, NMR is not suited for detection of kinetic intermediates. The complementary use of the two techniques provides a more precise and detailed picture of the folding process especially for multidomain proteins. Given recent advances in NMR that allow interpretable spectra to be obtained from larger proteins, we expect this combined strategy will prove to be generally useful.

ACKNOWLEDGMENT

We thank Professor D. Hoffman for providing us with the coordinates of L9 prior to publication and for helpful discussions. We also thank Professor D. Hoffman for generously providing us with the *E. coli* strains for the production of L9.

REFERENCES

1. Lillemoen, J., Cameron, C. S., and Hoffman, D. W. (1997) *J. Mol. Biol. 268*, 482−493.
2. Hoffman, D. W., Cameron, C. S., Davies, C., White, S. W., and Ramakrishnan, V. (1996) *J. Mol. Biol. 264*, 1058−1071.

3. Hoffman, D. W., Davies, C., Gerchman, S. E., Kycia, J. H., Porter, S. J., White, S. W., and Ramakrishnan, V. (1994) *EMBO J. 13*, 205−212.
4. Kuhlman, B., Yang, H. Y., Boice, J. A., Fairman, R., and Raleigh, D. P. (1997) *J. Mol. Biol. 270*, 640−647.
5. Jackson, S. E. (1998) *Folding Des. 3*, R81−R91.
6. Fersht, A. R. (1997) *Curr. Opin. Struct. Biol. 7*, 3−9.
7. Huang, G. S., and Oas, T. G. (1995) *Biochemistry 34*, 3884−3892.
8. Jackson, S. E., and Fersht, A. R. (1991) *Biochemistry 30*, 10436−10443.
9. Abkevich, V. I., Gutin, A. M., and Shakhnovich, E. I. (1995) *Protein Sci. 4*, 1167−1177.
10. Price, N. C. (1994) in *Mechanisms of Protein Folding* (Pain, R. H., Ed.) Oxford University Press, Oxford, U.K.
11. Jaenicke, R. (1991) *Biochemistry 30*, 3147−3161.
12. Kuhlman, B., Boice, J. A., Fairman, R., and Raleigh, D. P. (1998) *Biochemistry 37*, 1025−1032.
13. Kuhlman, B., Luisi, D. L., Evans, P. A., and Raleigh, D. P. (1998) *J. Mol. Biol. 284*, 1661−1670.
14. Huang, G. S., and Oas, T. G. (1995) *Proc. Natl. Acad. Sci. U.S.A. 92*, 6878−6882.
15. Wu, W. J., and Raleigh, D. P. (1998) *Biopolymers 45*, 381−394.
16. Evans, P. A., Kautz, R. A., Fox, R. O., and Dobson, C. M. (1989) *Biochemistry 28*, 362−370.
17. Dobson, D. M., and Evans, P. A. (1984) *Biochemistry 23*, 4267−4270.
18. Pace, C. N., Shirley, B. A., and Thomson, J. A. (1990) in *Protein Structure: A Practical Approach* (Creighton, T. E., Ed.) Oxford University Press, Oxford, U.K.
19. Sandstrom, J. (1982) *Dynamic NMR Spectroscopy*, Academic Press, London.
20. Campbell, I. D., Dobson, C. M., Ratcliffe, R. G., and Williams, R. J. P. (1978) *J. Magn. Reson. 29*, 397−417.
21. Roder, H. (1989) *Methods Enzymol. 176*, 446−473.
22. Shoemaker, D. P., Garland, C. W., and Nibler, J. W. (1989) *Experiments in Physical Chemistry*, 5th ed., McGraw-Hill Inc, New York.
23. Kuhlman, B., and Raleigh, D. P. (1998) *Protein Sci. 7*, 1−8.
24. Myers, J. K., Pace, C. N., and Scholtz, J. M. (1995) *Protein Sci. 4*, 2138−2148.
25. Tanford, C. (1970) *Adv. Protein Chem. 24*, 1−95.
26. Kim, D. E., Gu, H., and Baker, D. (1998) *Proc. Natl. Acad. Sci. U.S.A. 95*, 4982−4986.
27. Kraulis, P. J. (1991) *J. Appl. Crystallogr. 24*, 946−950.

BI9830314